Journal of the European Ceramic Society **15** (1995) 435–443

0955-2219/95/$9.50

Thermal Conductivity Improvement of YAG Added AlN Ceramics in the Grain Boundary Elimination Process

Mitsuo Kasori & Fumio Ueno

Materials & Devices Research Laboratory, Research & Development Center, Toshiba Corporation, Kawasaki, Kanagawa 210, Japan

(Received 26 August 1993; revised version received 14 July 1994; accepted 10 August 1994)

Abstract

The primary cause of the thermal conductivity improvement in Y_2O_3-containing AlN ceramics caused by elimination of the grain boundary phase was investigated. $Y_3Al_5O_{12}$ (YAG)-containing AlN powder compacts were sufficiently densified by firing at 1800°C for 30 min, but had low thermal conductivity (90–110 Wm^{-1} K^{-1}). Improvement to 245 Wm^{-1} K^{-1} and elimination of the grain boundary phases was brought about by annealing in a carbo-reductive atmosphere at 1850°C for up to 100 h. During annealing, $YAlO_3$, $Y_4Al_2O_9$ and Y_2O_3 appeared as a result of the reduction–nitridation of the Al_2O_3 constituent in the YAG. Subsequently, these yttrium rich phases acted as oxygen getters for the dissolved Al_2O_3 which was originally included in the AlN grains. The Al_2O_3 continuously changed into AlN by reduction–nitridation. The cyclic oxygen removal from the AlN through the grain boundary phase composition change is seen as the primary cause for the thermal conductivity improvement.

1 Introduction

AlN ceramic is an insulator having a high thermal conductivity. Applications of AlN ceramics for high power devices and micro electronics packaging materials as heat dissipation substrates are spreading.[1] The heat carrier in AlN is the phonon. Phonon scattering may occur from impurities or lattice imperfections and decrease thermal conductivity. The most harmful impurity has been found to be oxygen. Dissolved oxygen ions in AlN occupy the nitrogen sites, and they generate Al vacancies to compensate the electric charge balance.[2] Commercially available AlN powders have around 1 wt% of oxygen as a surface layer of oxide or oxy-nitride of aluminum.[3,4] Without any oxygen getter, the oxygen in the surface layer dissolves into AlN during sintering. A full densification of AlN by pressureless sintering has been achieved by rare earth or alkaline earth additions.[5] Y_2O_3 and CaO are popular sintering aids. These sintering aids react with the aluminum oxide surface layer at a sintering temperature of around 1800°C. These reactions generate yttrium aluminate or calcium aluminate liquid phases during sintering. These liquid phases are supposed to promote liquid phase sintering of AlN. The aluminates remain in the ceramics as grain boundary phases after sintering. In this way, these sintering aids act as oxygen getters by fixing aluminum oxide as a grain boundary phase. In the case of Y_2O_3 additions, $Y_3Al_5O_{12}$ (YAG), $YAlO_3$(YAL), $Y_4Al_2O_9$ (YAM), and Y_2O_3 were found as grain boundary phases. The kinds of phases remaining depend on the ratio of the amount of oxygen in the starting AlN powder and the amount of Y_2O_3 addition.

Prolonged firing of up to 96 h in a carbo-reductive atmosphere is known to improve thermal conductivity up to around 260 Wm^{-1} K^{-1}.[6] With this kind of firing, the yttrium aluminate grain boundary phases are eliminated from the AlN ceramic. The rate of grain boundary phase elimination from the ceramic is higher when it is fired in a graphite setter than when fired in an AlN setter. A trace amount of carbon gas from the setter or from a graphite heater promotes the reduction–nitridation of the oxides in the yttrium aluminate phases at the ceramic surface. An oxide concentration gradient between the surface and the interior of the ceramics develops during firing; it relaxes by grain boundary diffusion of the oxide.[6] This kind of thermal conductivity improvement and grain boundary elimination has also been observed in other lanthanoide additions but not in alkaline earth additions.[7,8]

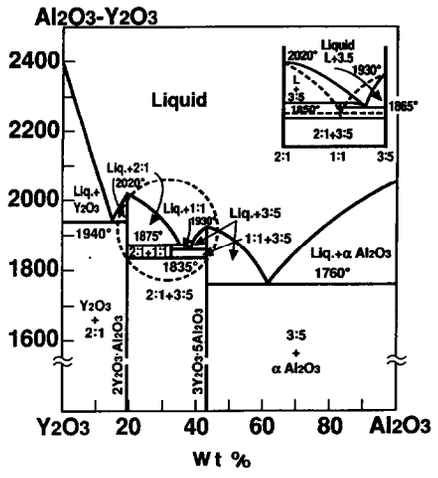

Fig. 1. Phase diagram of Al_2O_3–Y_2O_3 system.

The influence of the grain boundary phase on thermal conductivity has been considered to be slight.[9,10] This is because the grain boundary phases are located at three grain points, thus maintaining sufficient AlN–AlN contacts. AlN grain growth in the ceramics has also been observed in prolonged firing. However, the mean free path of phonons in AlN at room temperature has been estimated to be around 10–30 nm,[11] and the average grain size of AlN in the ceramics is at least around 3 μm even before the prolonged firing. Namely, the mean free path is sufficiently small for the AlN grain size and phonon scattering at the AlN–AlN grain boundaries to have a negligible influence on thermal conductivity.

The aim of this work was to clarify the primary cause of the thermal conductivity improvement in the grain boundary elimination process. The authors have considered that a further oxygen removal from the AlN grains by yttrium aluminates or yttrium oxide grain boundary phases during the grain boundary elimination process might be the primary cause. YAG was used as a sintering aid to test this hypothesis. It was considered from the Y_2O_3–Al_2O_3 phase diagram shown in Fig. 1[12] that YAG should act as a sintering aid if a YAG-containing AlN powder compact is fired at a higher temperature than the liquidus temperature of the YAG. It was also considered that the AlN ceramics densified by YAG addition should have a higher concentration of dissolved oxygen than AlN ceramics densified with Y_2O_3 addition. We can obtain AlN ceramics having a certain amount of dissolved oxygen and having YAG grain boundary phase by this method. Firings of the YAG-containing AlN ceramics in a carbo-reductive atmosphere can be expected to reveal the primary cause of the thermal conductivity improvement in the grain boundary elimination process.

2 Experimental Procedure

2.1 Ceramic preparation

Fine powders of Y_2O_3 (Shinestu Chemical, 4N) an α-Al_2O_3 (Baikowski, 4N) were mixed at a ratio of $3Y_2O_3:5Al_2O_3$. After 0·5 wt% AlF_3 fine powder (Morita Kagaku Kogyo, 3N) was added as a catalyst, the mixed powder was heated at 1500°C for 5 h in an alumina crucible in air. It was then pulverized using an Al_2O_3 mortar. The composition was identified as YAG by XRD. AlN mixed powders, (Tokuyama Soda, F-type, oxygen 0·71 wt%), containing 1, 2, 5, 10, and 20 wt% YAG were prepared. AlN mixed powders containing 1 and 3 wt% Y_2O_3 were also prepared. The mixing was carried out by a wet ball mill using butyl alcohol. After adding a 5 wt% acrylic binder (Tyukyo Oil, SERUNA-SE3000), the mixed powders were fabricated into 30 × 30 × 8 mm compacts by pressing under 50 MPa. Then, they were de-waxed by heating at up to 700°C in N_2 gas.

The mixed powder compacts were sintered at 1800°C for 30 min, in a h-BN setter under an atmospheric pressure of nitrogen using a graphite heater furnace. These ceramics were then annealed at 1850°C for 1, 3, 10, 30, and 100 h respectively, in a graphite setter under an atmospheric pressure of nitrogen in the same graphite heater furnace.

2.2 Characterization

The thermal diffusivity at 23 ± 2°C was measured by the laser-flash method (Shinku Riko, TC-3000). A ruby laser was used for the flash and InSb was used for the infrared detector. Disk samples having 10 mm diameter and around 3·5 mm thickness were coated with a thin gold layer on the surface to prevent the flash penetrating into the ceramics. A carbon black layer was applied over the gold layer to enhance the absorption of the flash energy. Corrections on thermal diffusivity regarding the flash duration time and flash inhomogeneity were carried out according to the Japanese Industrial Standard (JIS-R1611). The thermal conductivity was calculated from the thermal diffusivity, the specific heat measured by differential scanning calorimetry, and the density.

The constituents of the ceramics were identified by powder XRD after being pulverized. The *c*-axis lengths of AlN at room temperature were measured using the internal standard for Si (NIST, 640b). The yttrium contents in the ceramics were measured by the inductively coupled plasma (ICP) method.

Table 1. Comparisons of yttrium concentrations between starting powder compositions and ceramics by ICP.

		Yttrium concentration/wt%	
Additives	*(wt%)*	*Starting composition*	*Analytical result*
YAG	20	8·99	9·03
	10	4·49	3·73
	5	2·25	2·11
	1	0·45	0·44
Y_2O_3	3	2·36	2·26

3 Results

3.1 Sintering by YAG additions

The AlN mixed powder compacts fired at 1800°C–30 min were sufficiently densified without any pores. Table 1 shows the yttrium concentrations in the ceramics measured by ICP and those calculated from the starting compositions. The constituents of the ceramics besides AlN were YAG for YAG added, YAG for 1 wt% Y_2O_3 added, and YAL and YAM for 3 wt% Y_2O_3 added. Figure 2 shows the relationships between the density, the thermal conductivity and the amount of YAG or Y_2O_3 additions. The density increased linearly with the amount of additions in both cases. The thermal conductivity decreased as the amount of YAG addition increased. On the other hand, the thermal conductivity improved as the amount of Y_2O_3 addition increased.

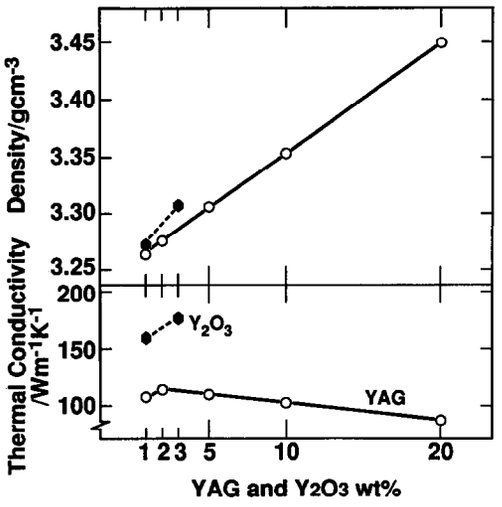

Fig. 2. Relationship between thermal conductivity and density of ceramics and amount of YAG or Y_2O_3 additions.

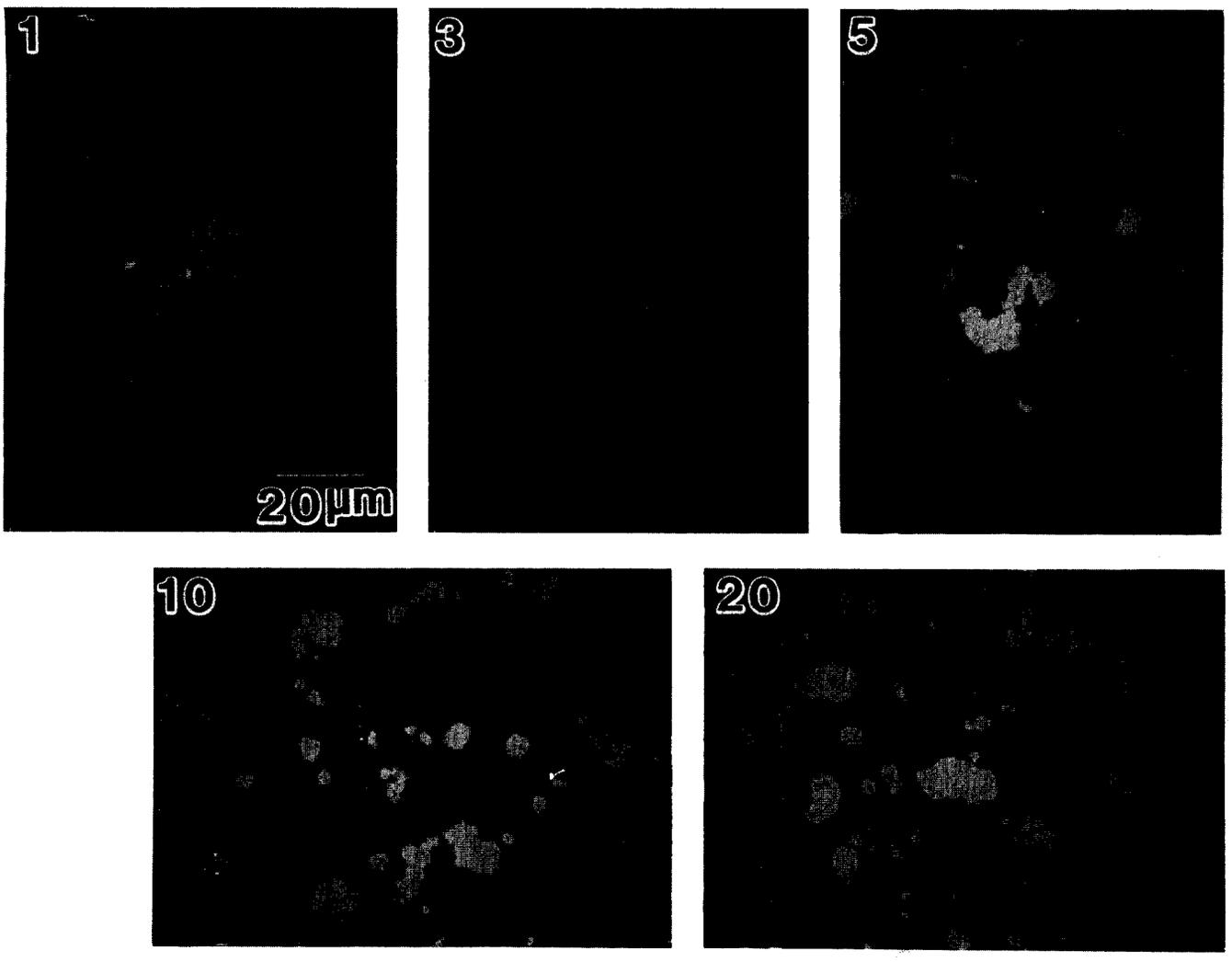

Fig. 3. SEM photographs of polished surfaces of YAG added ceramics.

Considering that the thermal conductivity of the AlN ceramics using Tokuyama Soda F-Type powder which has no additives and have at least 98% theoretical density ranged from 90 to 120 Wm^{-1} K^{-1},[6,13,14] it was considered that the YAG additions contributed to densification but not to thermal conductivity improvement. The thermal conductivity of YAG is around 13 Wm^{-1} K^{-1}.[15] Therefore, the decrease in thermal conductivity by YAG addition is considered to be the result of increase in the amount of poorly conducting phase (YAG) for a given oxygen content in the AlN.[16]

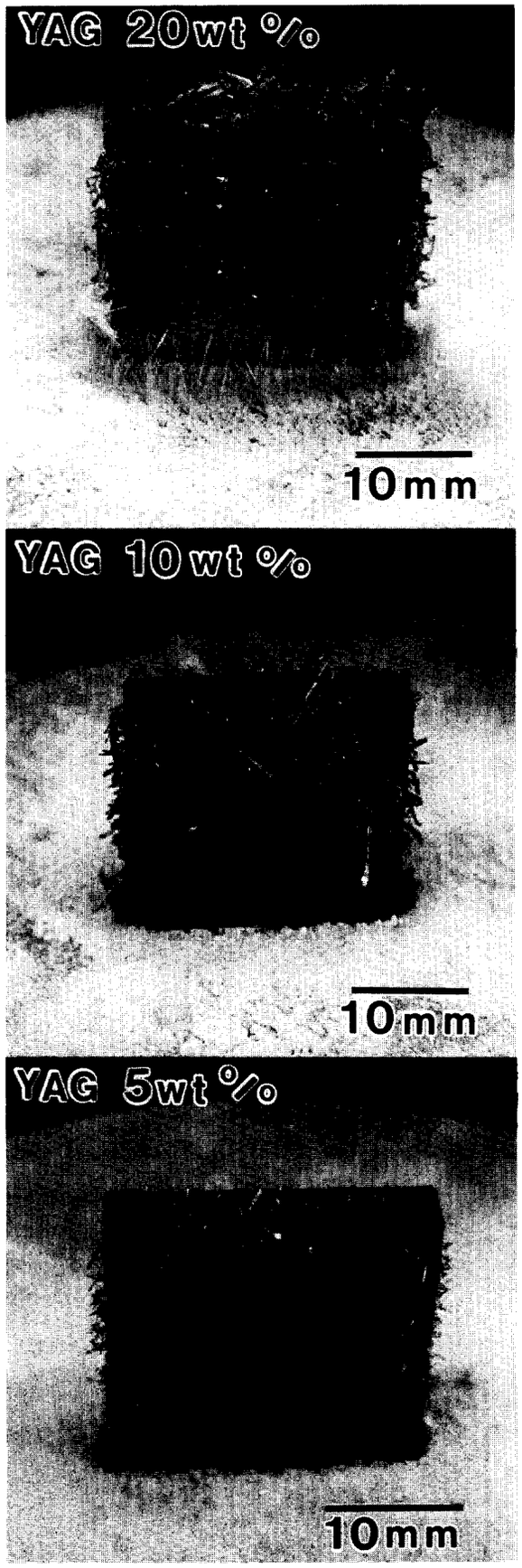

Fig. 4. Annealed appearances of ceramics after 10 h annealings.

The YAG distributions in individual ceramics are shown in Fig. 3. The photographs are SEM images of polished surfaces, and the individual numbers in the photographs represent the amount of YAG addition. The white parts can be attributed to the YAG regions. YAG was distributed as islands ranging from 1 to 20 μm in diameter in the AlN matrix except for the 3 wt% YAG added case. The ratio of $Al_2O_3/(Al_2O_3 + Y_2O_3)$ in the YAG 3 wt% addition case was 0·63, a value very close to the eutectic point composition of Y_2O_3–Al_2O_3. The amount of Al_2O_3 was calculated from YAG and the oxygen content of AlN starting powder.

3.2 Thermal conductivity improvement by annealing in the carbo-reductive atmosphere

The appearances of the as-annealed ceramics are shown in Fig. 4. The photographs show the samples of 5, 10, and 20 wt% YAG, respectively, after 10 h annealing. Needle-like AlN crystals and a black layer on the ceramic surfaces were observed in all cases. The black layer consisted of YN and AlN as determined by XRD. The needle-like AlN crystals grew larger as the YAG content became higher.

Figure 5 shows the relationship between the weight changes of the ceramic constituents besides AlN and the annealing time. The weights were calculated based on the weights of the pre-annealed ceramics, i.e. weight change (%) = (weight before annealed–weight after annealed)/(weight

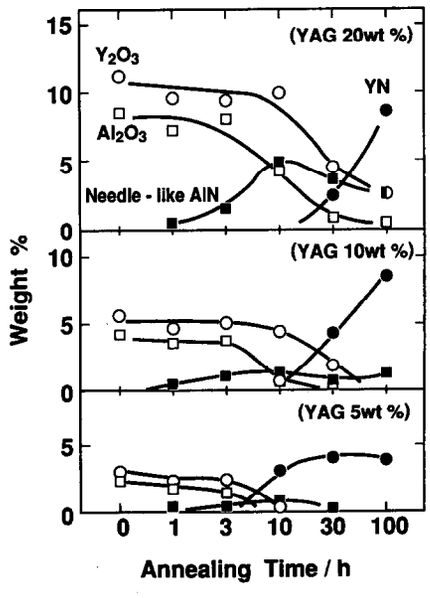

Fig. 5. Weight changes of secondary ceramic constituents during annealings.

before annealed) × 100. The weight changes of the Y_2O_3 and the Al_2O_3 constituents are commensurate with the composition changes of the yttrium aluminate grain boundary phases. The amount of the yttrium aluminate phases were measured from XRD peaks using calibration curves made in advance. Figure 6 shows the yttrium concentrations in the ceramics measured from the ICP and XRD peaks. There was little difference between them. As shown in Fig. 5, the amount of the needle-like AlN crystals increased as the Al_2O_3 constituent in the yttrium aluminate grain boundary phase decreased. The amount of YN also increased as Y_2O_3 constituent in the yttrium aluminate grain boundary phase decreased. From these results, it is considered that the Al_2O_3 constituent in the YAG changed into the needle-like AlN and the Y_2O_3 constituent changed into YN. The amount of the needle-like

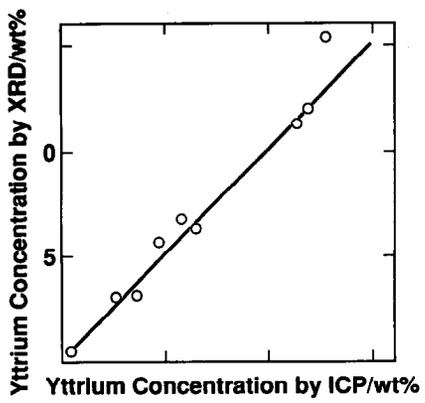

Fig. 6. Comparison of yttrium concentrations in AlN ceramics measured by ICP and XRD.

AlN crystal was maximized at 10 h and decreased over 30 h. It was considered that the enlargement of the surface area by the needle-like AlN crystal generation brought about a substantial sublima-

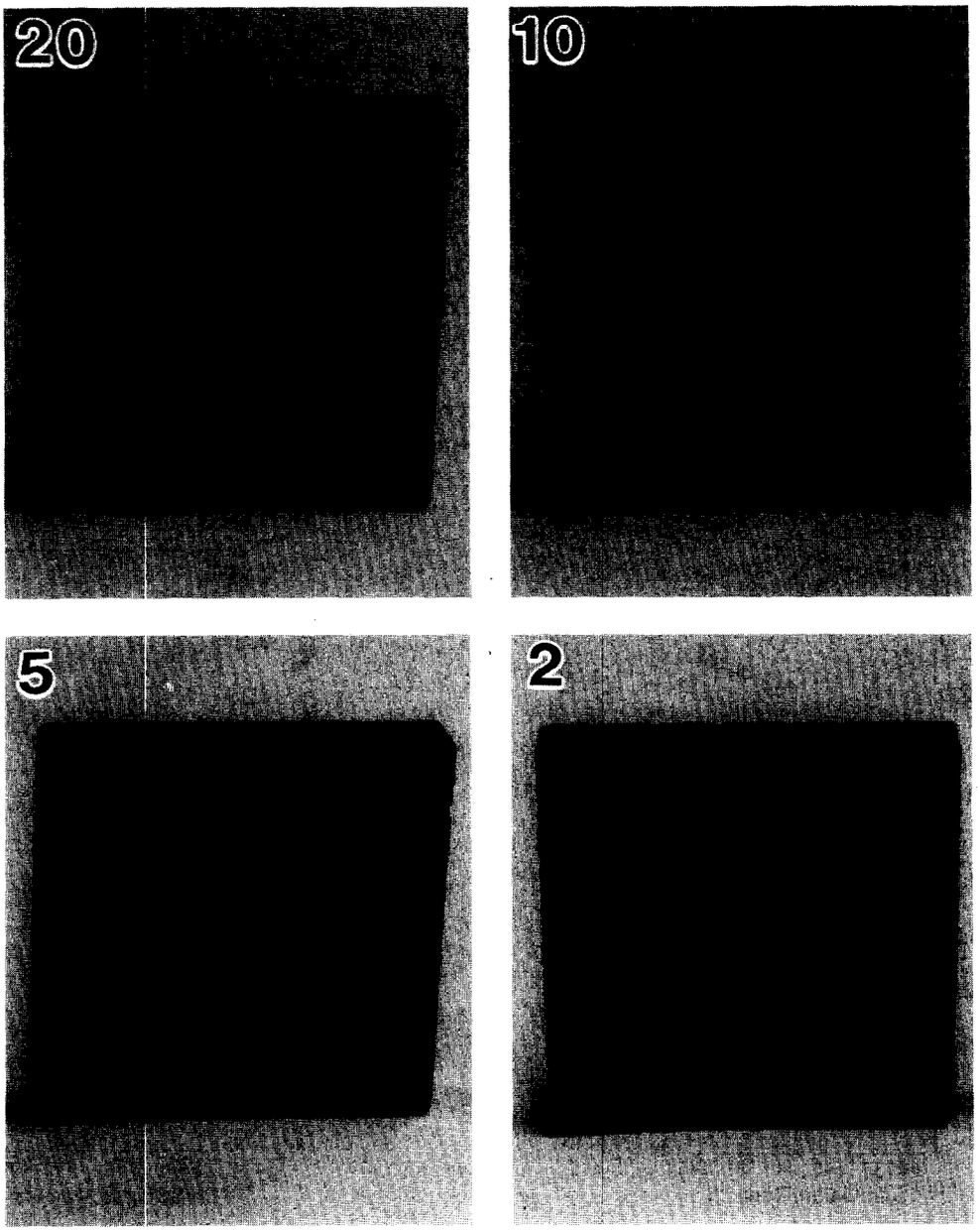

Fig. 7. AlN ceramics surfaces after 3 h annealings. Needle-like AlN crystals were eliminated.

		Firing Time/h					
		0	1	3	10	30	100
YAG	20 wt%	YAG19.7	YAG16.8	YAG15.5 YAP4.5	YAP 9.5 YAM 7.2	YAM 4.5 Y_2O_3 3.1	YAM 1.3 Y_2O_3 2.1
	10	YAG9.9	YAG8.5	YAG6.0 YAP4.1	YAM 4.5 Y_2O_3 0.8	YAM 1.3 Y_2O_3 0.8	
	5	YAG5.3	YAG4.1	YAG1.4 YAP2.4	YAM 0.3 $Y_2O_3$0.02		
	2	YAG1.6	YAG1.6	YAG0.7			
	1	YAG0.8	YAG0.7				
Y_2O_3	3	YAP2.7 YAM2.6					
	1	YAG2.7					

Fig. 8. Interior grain boundary phases changes of AlN ceramics during annealings. Blanks present grain boundary free.

tion of AlN. The YN generation on the ceramic surfaces was striking for the ceramics having lesser YAG contents. The appearances of the ceramics after 3 h annealings are shown in Fig.7. The needle-like AlN crystals were taken off beforehand in these cases. The YN layer covered the whole ceramic surfaces in the case of 1 and 2 wt% YAG additions. Only the upper side of the ceramics was covered with the YN layer, in the case of 5 wt% YAG addition. There was no YN layer on the ceramic surfaces in the case of 10 and 20 wt% YAG additions. It was observed that parts near to the graphite setter tended to form YN quickly.

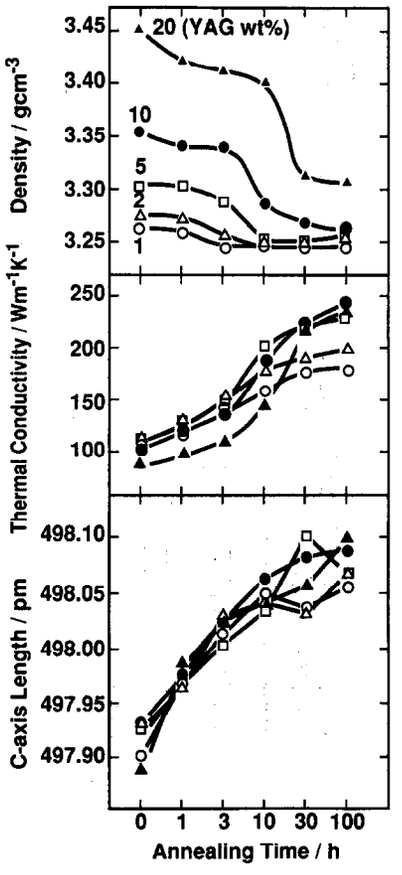

Fig. 9. Relationship between density, thermal conductivity, *c*-axis length and annealing time in different YAG additions.

It was not only the surface layer, but also the interior compositions of the ceramics that were changed during the annealing. It was expected that the grain boundary phase compositions in the vicinity of the ceramic surface were different from the interior.[17] A layer at least 0·5 mm thick was cut from the surface before pulverizing for the XRD measurements. The grain boundary compositions changed during the annealing, as shown in Fig. 8. Blanks indicate the absence of grain boundary phase examined by XRD. YAG turned into phases richer in yttrium as the annealing time was prolonged. Namely, the grain boundary phases changed in the direction of YAG→YAP→YAM→Y_2O_3. Ceramics having a lower YAG content reached the grain boundary phase free state quicker. The grain boundary phases were eliminated completely after 100 h annealing except for YAG 20 wt% addition.

The relationship of the density, the thermal conductivity and the *c*-axis length of AlN to the annealing time is shown in Fig. 9. The numbers in the figure represent the YAG content. The density converged to the theoretical density of AlN (3·26 gcm^{-3}) as the annealing time increased because of the elimination of grain boundary phases with higher densities than AlN. The smaller amount of YAG content made the density decrease earlier. The density decreased in a different manner to the YAG contents. The density decreased noticeably during 10–30 h for 20 wt%, 3–10 h for 10 and 5 wt% and 1–3 h for 2 and 1 wt% YAG. The thermal conductivity improved almost linearly in YAG 1 and 2 wt%. Thermal conductivity improvement

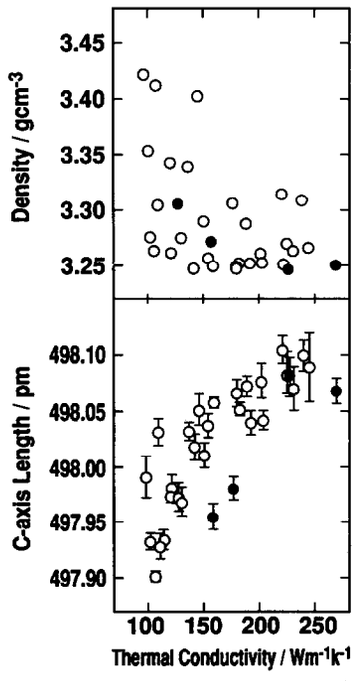

Fig. 10. Relationship between density, *c*-axis length of AlN and thermal conductivity.

occurred during 10–30 h for YAG 20 wt% and 3–10 h for YAG 10 and 5 wt%. These periods coincided with the period of decreasing density. On the other hand the *c*–axis length lengthened gradually during the annealing. Standard deviation of each of the *c*–axis lengths was within 0·10 pm. The *c*–axis lengths ranged from 497·89 to 497·93 pm before annealing and then ranged from 498·07 to 498·10 pm. The *c*–axis length of starting AlN powder was 498·05. The *c*–axis length became shorter at sintering and was then restored by annealing.

In Fig. 10 the relationship between thermal conductivity, density and the *c*–axis length for all samples in this study are shown. The open and the solid circles indicate YAG and Y_2O_3 added, respectively. Even though the density is almost the theoretical of AlN, the thermal conductivity ranged from 90 to 260 $Wm^{-1}\ K^{-1}$. The wide extent of the density range was diminished as the thermal conductivity increased. The *c*–axis length increased as thermal conductivity rose. However, it was found that, a coefficient of correlation to the thermal conductivity was different around the upper and the lower sides of 150 $Wm^{-1}\ K^{-1}$.

Thermal conductivity increased from around 100 to around 250 $Wm^{-1}\ K^{-1}$ by annealing. The *c*–axis length also increased from around 497·3 to 498·8 pm. The highest thermal conductivity within the scale of experiment was 265 $Wm^{-1}\ K^{-1}$. This was obtained by 3 wt% Y_2O_3 addition and 30 h annealing. In the case of YAG additions, the highest was 245 $Wm^{-1}\ K^{-1}$ for 10 wt% YAG after 100 h firing.

4 Discussion

Oxygen occupies nitrogen sites when it dissolves into AlN. The dissolution generates Al vacancies to preserve the electric charge balance. An increase in Al vacancy concentration decreases the *c*–axis.[18] The *c*-axis length of the starting AlN powder was 498·05 ± 0·015 pm. From the results of the *c*–axis length and the thermal conductivity changes, it was considered that the oxygen first dissolved into AlN at 1800°C–30 min sintering and was then gradually removed from the AlN grains by the annealings. Trace amounts of carbon gases are expected in the firing atmosphere. The carbon gas should stimulate the reduction–nitridation of oxides at a high temperature in a nitrogen atmosphere. Therefore, Al_2O_3 and Y_2O_3 in the yttrium aluminate were changed into AlN and YN, respectively, as in the following equations.

$$Al_2O_3 + N_2 + 3C \rightarrow 2AlN + 3CO\uparrow (-40\text{k mol}^{-1}) \quad (1)$$

$$Y_2O_3 + N_2 + 3C \rightarrow 2YN + 3CO\uparrow (80\text{k mol}^{-1}) \quad (2)$$

The YAG located at the ceramic surface reacted with the carbo-reductive atmosphere directly. Subsequently, the Al_2O_3 in the YAG located at the surface changed into AlN according to reaction (1) as a first stage. An oxide concentration gradient between the surface and the interior of the ceramics developed, and was then relaxed by the grain boundary diffusion of the oxide.[6]

The consumption of the Al_2O_3 constituent in the YAG and other yttrium aluminates formed yttrium richer phases, as in the following equations.

$$Y_3Al_5O_{12} + N_2 + 3C \rightarrow 3YAlO_3 + 2AlN + 3CO\uparrow \quad (3)$$

$$4YAlO_3 + N_2 + 3C \rightarrow Y_4Al_2O_9 + 2AlN + 3CO\uparrow \quad (4)$$

$$Y_4Al_2O_9 + N_2 + 3C \rightarrow 2Y_2O_3 + 2AlN + 3CO\uparrow \quad (5)$$

These yttrium rich phases should react with dissolved oxygen in the AlN grain as follows.

$$2Y_2O_3 + Al_2O_3 \rightarrow Y_4Al_2O_9 \quad (6)$$

$$Y_4Al_2O_9 + Al_2O_3 \rightarrow 4YAlO_3 \quad (7)$$

$$3YAlO_3 + Al_2O_3 \rightarrow Y_3Al_5O_{12} \quad (8)$$

The dissolved oxygen in the AlN grains was removed gradually and the thermal conductivity was improved by annealing. The relationship between thermal conductivity and the *c*–axis in Figs 9 and 10 is in agreement with this interpretation, as is the remarkable thermal conductivity improvement at the period of the notable density drop. The reduction–nitridation of the Al_2O_3 at the notable density drop period must be vigorous. The thermal conductivity increase after the grain boundary phase free was believed to be attributed by further oxygen removal with a small amount of yttrium compound less than several hundred ppm.

It is considered that the changes in the yttrium aluminate phase compositions during the annealings were caused by the difference between the reduction–nitridation rate of Al_2O_3 and Y_2O_3 in the YAG. In the case of eqn (2), an excess amount of carbon was in the firing atmosphere, and because the CO gas is exhausted outside the furnace, the reaction should proceed toward the right side. The reactions presented in eqns (3)–(8) should occur simultaneously. It is expected that the migration of Al_2O_3 in the yttrium aluminate should be fast, because the yttrium aluminate was expected to be a liquid at the annealing temperature.[19]

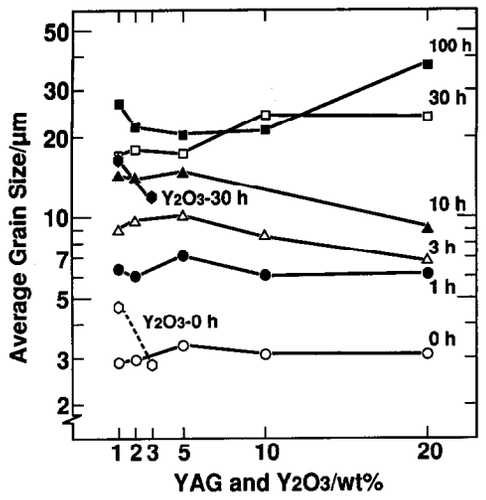

Fig. 11. Relationship between average grain size of AlN and amount of YAG or Y_2O_3 additions during annealings.

Equation (1) describes the AlN powder manufacturing method involving carbo–thermal reaction of Al_2O_3. It is interesting to ask whether oxygen removal without yttrium is possible or not. However, no thermal conductivity improvement was observed even though samples were annealed in the same way.[6,20] Figure 11 shows the grain growth of AlN during the annealings. The grains grew from around 3 μm to a range from 20 to 40 μm after 100 h annealing. One might expect the Al vacancies migrate to the grain boundaries during the grain growth. From the consideration of the mean free path of phonons in AlN, as mentioned earlier, the grain size itself is not directly related to thermal conductivity. Goto *et al.*[20] discussed that thermal conductivity has no relation to grain size ranging from 9 to 21 μm in phase free grain boundary AlN ceramics containing 500 ± 100 ppm oxygen. Watari *et al.*[21] also reported that no relationship was found between thermal conductivity and grain size from characterization of AlN ceramics that has an average grain size of between 4 and 40 μm and has 1·04–0·91 oxygen content.

It should be noted that before annealing, the thermal conductivity of 1 wt% YAG-containing ceramics was slightly lower than that of 3 wt% YAG-containing ceramic. A trace amount of oxygen removal might have occurred even for the 1800°C–30 min firing.

5 Conclusions

The thermal conductivity improvement of 260 Wm^{-1} K^{-1} grade-containing AlN ceramics can be divided into two processes. The first is fixing the original Al_2O_3 impurity in the AlN powder as a grain boundary phase. The second is the grain boundary elimination process by annealing in a carbo-reductive atmosphere. From evaluations on YAG-containing ceramics, we can obtain the conclusions listed below.

(1) The primary cause of thermal conductivity improvement in the grain boundary phase elimination process is considered to originate from a cyclic oxygen removal from the AlN grains by oxygen getters.

(2) The difference in the reduction–nitridation velocity between the Al_2O_3 and the Y_2O_3 constituents in the yttrium aluminate phases generates yttrium rich phase formation during annealing. The Al_2O_3 in the YAG changes into AlN at first. Consequently, yttrium rich phases are formed in the grain boundary phases and then they act as oxygen getters.

(3) Y_2O_3 is better for thermal conductivity than YAG. YAG has been found to be a sintering aid of AlN without any thermal conductivity improvement. The doping should be to form YAP and YAM for thermal conductivity.

References

1. Werdecker, W. & Aldinger, F., Aluminum Nitride—An alternative ceramic substrate for high power applications in micro circuits. *IEEE Trans. Compon., Hybrids. Manuf. Technol.*, 7(4) (1984) 399–404.
2. Slack, G. A., Nonmetallic crystals with high thermal conductivity. *J. Pys. Chem. Solids*, **34** (1973) 321–35.
3. Ponthieu, E., Grange, P., Delmon, B., Lonnoy, L., Leclercq, L., Bechara, R. & Grimblot, J., Proposal of a composition model for commercial AlN powders. *J. Europ. Ceram. Soc.*, **8** (1991) 233–41.
4. Dutta, I., Mira, S. & Rabenberg, L., Oxidation of sintered aluminum nitride at near-ambient temperature. *J. Am. Ceram. Soc.*, **75**(11) (1992) 3149–53.
5. Komeya, K., Inoue, H. & Tsuge, A., Effect of various additives on sintering of aluminum nitride. *Yogyo-Kyokai-shi*, **89**(6) (1981) 330–6, in Japanese.
6. Ueno, F. & Horiguchi, A., Grain boundary phase elimination and microstructure of aluminum nitride. *Proc. Ist. Europ. Soc. Conf. (ECerS'89)*, 1.383, 18–23 June 1989 Maastricht, The Netherlands.
7. Jackson, T. B., Virkar, A. V., More, K. L. & Cutler, R. A., The microstructure of aluminum nitride sintered with yttria. In presentation (11-E-90) of Am. Ceram. Soc. 92nd Annual Meet., 22–26 April, (1990) Dallas, Texas.
8. Horiguchi, A., Kasori, M., Ueno, F. & Tsuge, A., High thermal conductive AlN ceramics by pressureless sintering in reducing atmosphere — investigation of additives. *Proc. Annual Meeting Ceram. Soc. Japan*, 3HO3, 12–14 May 1987, Nagoya, Japan, in Japanese.
9. Lee, R. R., Development of high thermal conductivity aluminum nitride ceramics. *J. Am. Ceram. Soc.*, **74**(9) (1991) 2242–9.
10. Virkar, A. V., Jackson, T. B. & Cutler, R. A., Thermodynamics and kinetic effects of oxygen removal on the thermal conductivity of aluminum nitride. *J. Am. Ceram. Soc.*, **72**(11) (1989) 2031–42.

11. Slack, G. A., Tanzilli, R. A., Pohl, R. O. & Vandeersande, J. W., The intrinsic thermal conductivity of AlN. *J. Phys. Chem. Solids*, **4**(7) (1987) 641–7.
12. Toropov, N. A., Bonder, I. A., Galakhov, F. Ya., Nikogosyan, X. S. & Vinogradova, N. V., *Izu. Akad. Nauk SSSR, Ser. Khim., No. 7*, (1964) 1162. Printed in *Phase diagrams for Ceramists 1969 Supplement* Fig. 2344, Am. Ceram. Soc., (1969).
13. Kuramoto, N. & Taniguchi, T., Transparent AlN Ceramics. *J. Mater. Sci. Lett.*, **3** (1983) 471–4.
14. Kuramoto, N., Taniguchi, H. & Aso, I., Development of translucent aluminum nitride ceramics. *Ceram. Bull.*, **68**(4) (1989) 883–7.
15. Touloukian, Y. S., Powell, R. W., Ho, C. Y. & Klemens, P. G., *Thermophysical Properties of Matter*, Vol. 2 IFI/Plenum, New York-Washington, 1970.
16. Kingery, W. D., Thermal Conductivity: XIV, Conductivity of multicomponent systems. *J. Am. Ceram. Soc.*, **42**(12) (1959) 617–27.
17. Yagi, T., Shinozaki, K., Kato, M., Sawada, Y. & Mizutani, N., Migration of grain boundary phases of AlN ceramics in joined sample of sintered and hot-pressed body. *J. Ceram. Soc. Japan*, **98**(2) (1990) 198–203, in Japanese.
18. Adams, I., AuCoin, T. R. & Wolff, G. A., Luminescence in the system Al_2O_3–AlN. *J. Electrochemical Soc.*, **109**[11] (1962) 1050–4.
19. Yamashita, Y., Shinozaki, K. & Mizutani, N., The temperature measurement of the liquid phase formation in AlN–Y_2O_3 (CaO)–Al_2O_3 system using a self-made high temperature DTA. *Proc. Annual Meeting, Ceram. Soc. Japan.*, 3C05, 5–7 April, 1993, Tokyo, Japan, in Japanese.
20. Goto, Y., Ueno, F., Kasori, H. & Horiguchi, A., The relation between oxygen content of aluminum nitride and its thermal conductivity. *Proc. Annual Meeting, Ceram. Soc. Japan.*, 1A10, 23–25 May 1990, Kobe, Japan, in Japanese.
21. Watari, K., Ishizaki, K. & Fujikawa, T., Thermal conduction Mechanism of Aluminum nitride ceramics. *J. Mater. Sci.*, **27** (1992) 2627–30.